"SEEING" THROUGH FLOWS IN LANGLEY'S
0.3-METER TRANSONIC CRYOGENIC TUNNEL

W. L. Snow, A. W. Burner, and W. K. Goad
NASA Langley Research Center
Hampton, Virginia 23665

INTRODUCTION

Cryogenic wind tunnels are being developed to enable testing at realistic Reynolds numbers. Such facilities take advantage of the increasing density and decreasing viscosity associated with cooling. When coupled with high pressure operation, these tunnels can provide aeronautical engineers with full scale Reynolds number simulation. The high dynamic pressures available in many of these test environments coupled with reasonable large and slender models can effect considerable deformation. Wing tips are expected to deflect 2 to 3 inches over 30 inch spans for some configurations in the NTF. The test engineer is faced with the dilemma of having unique data on an unknown model geometry unless ancillary measurements can provide simultaneous topological information. Virtually all of the proposed techniques being considered to discern model deformation including stereo photogrammetry, moiré topology, or surface LED trackers presume that identifiable targets can be viewed clearly and unambiguously thru the flow field. The tests described herein were made to shed light on these problems and were conducted in the Langley 0.3-Meter Transonic Cryogenic Tunnel.

IDEALIZED TARGET PROFILES

For purposes of modelling the problem, it is convenient to represent the ideal target as a rectangular distribution of energy (or image density). When viewed under less than ideal circumstances the distribution will in general shift and or become diffuse as suggested in figure 1. These effects directly influence the accuracy of model deformation data.
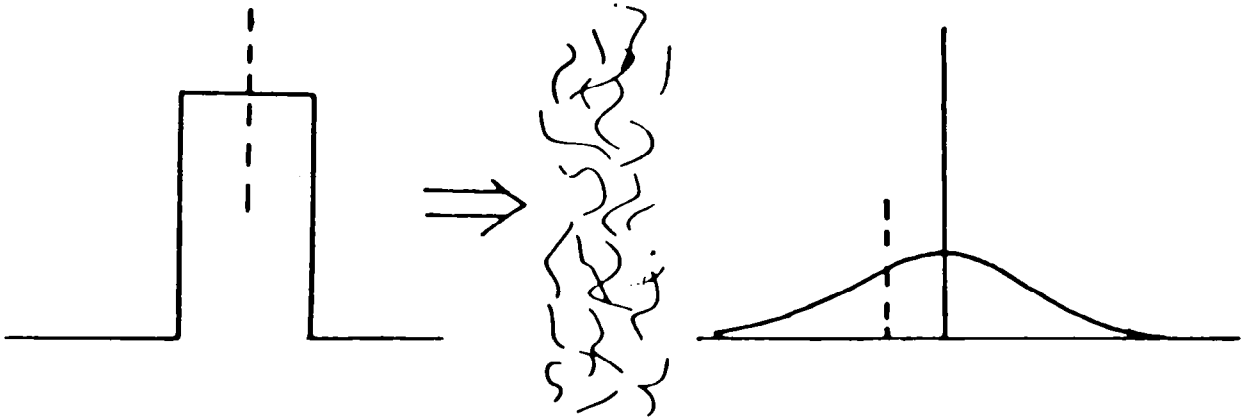

Figure 1

EFFECT OF CONDENSATION OVER AIRFOIL

Condensation and turbulence are potential problem areas. Cryogenic facilities work close to the condensation line to maximize the cryogenic advantage. Figure 2 shows the effect as saturation is increased by holding pressure constant and decreasing temperature. These areas will be avoidable by effective use of the operating envelope of the facility. As the condensation curve is approached, say by holding pressure constant and decreasing temperature, then 'fog' begins to appear. This is shown in figure 2 with density increasing from (a) to (d) with case (d) representing complete 'white out' as the liquid-vapor curve is crossed.
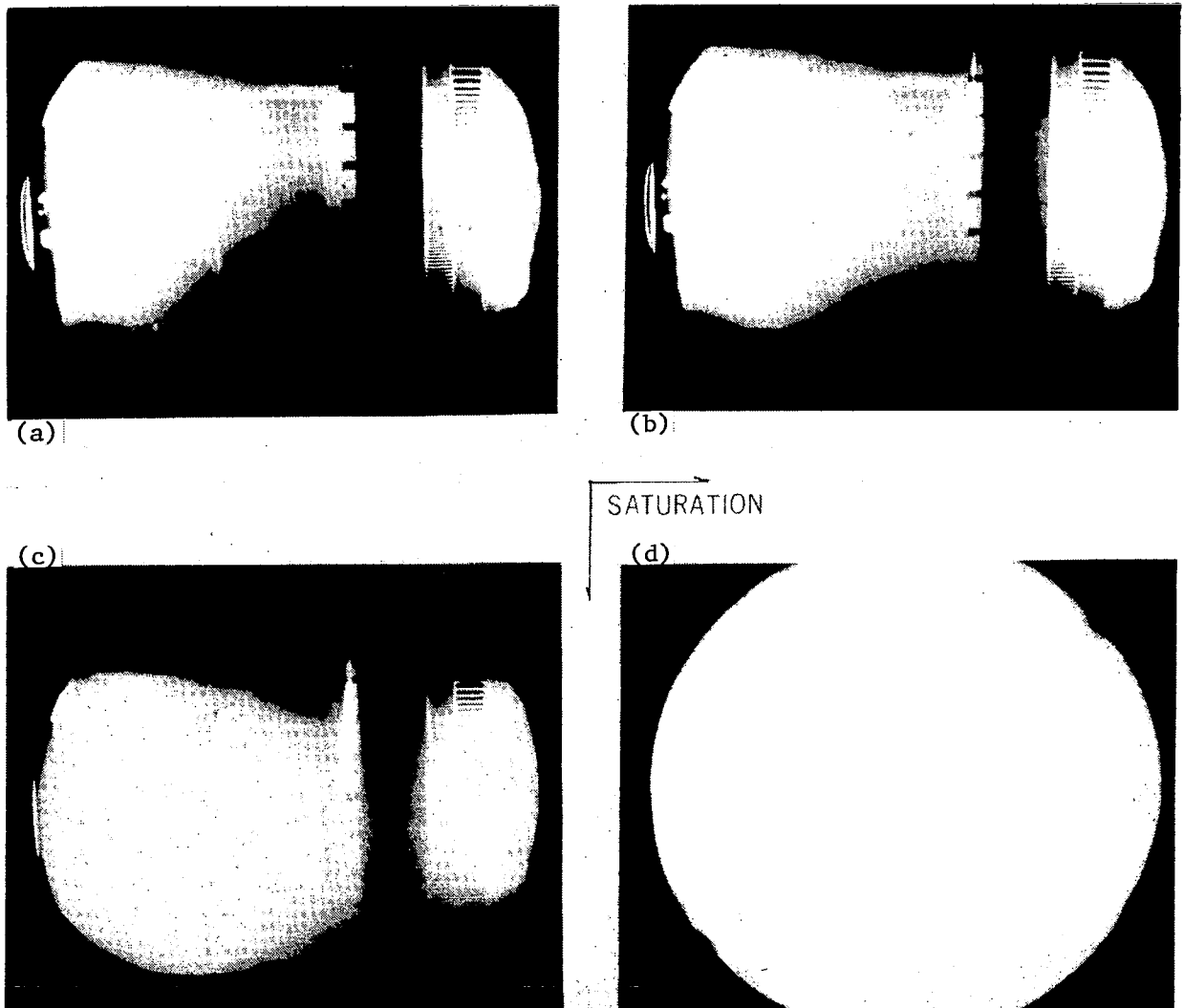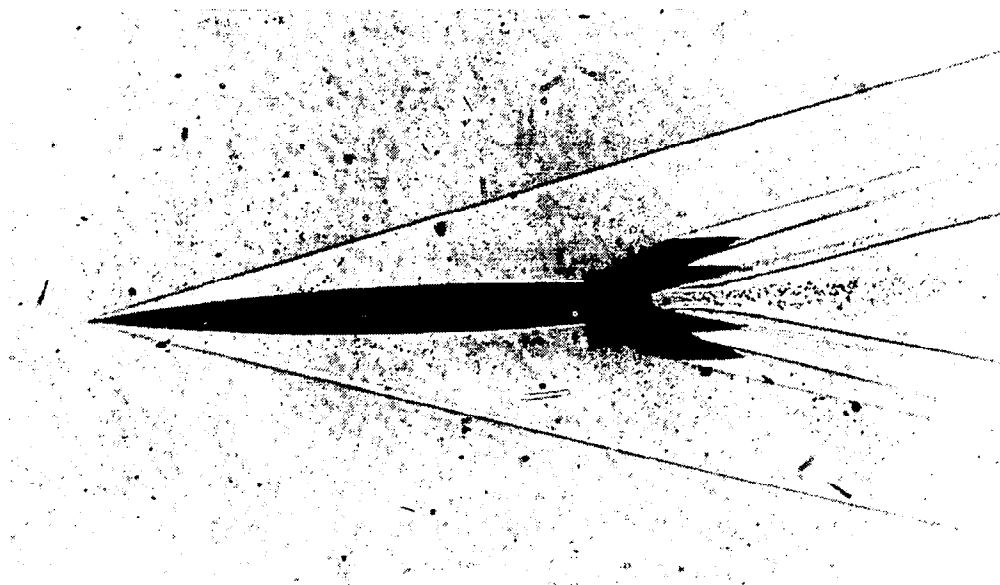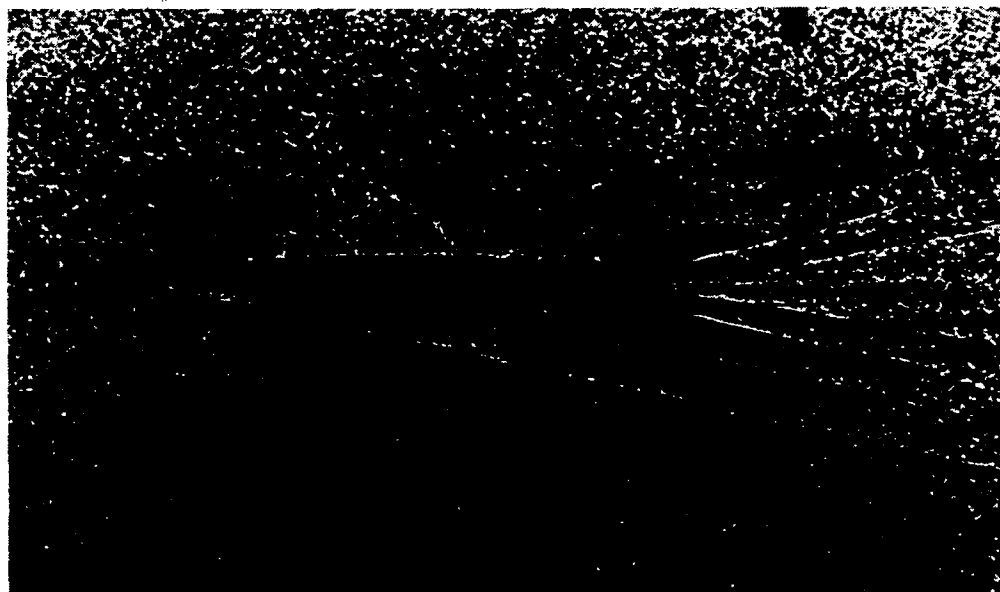

(a)

(b)

SATURATION

(c)

(d)

Figure 2

EFFECTS OF TURBULENT BOUNDARY LAYERS

Turbulence as suggested in figure 3 will be less forgiving and unavoidable. These photos from NACA RM A56B21 show focussed shadowgraphs for still air (a) and in the presence of flow induced turbulent boundary layers (b). Boundary layer effects will undoubtedly impose limits to image quality and will be assessed for NTF during the shakedown testing.

(a) Tunnel Mach number = 0; missile Mach number = 1

(b) Tunnel Mach number = 2; missile Mach number = 5

Figure 3

PHOTOGRAPHY THROUGH THE SIDE WINDOWS

To quantitatively assess image quality, the Modulation Transfer Function (MTF) of the optical designer is used. An image can be decomposed into its two dimensional Fourier spatial frequencies. The MTF is a plot of the relative efficiency of the system to pass these frequencies. To measure the response, a logarithmically increasing density of bars (Sayce target) is photographed through the flow as shown in figure 4. The diffusely illuminated target is viewed through the flow using a 70 mm camera with telephoto lens. Equipment is housed in sidemounted schlieren pods.
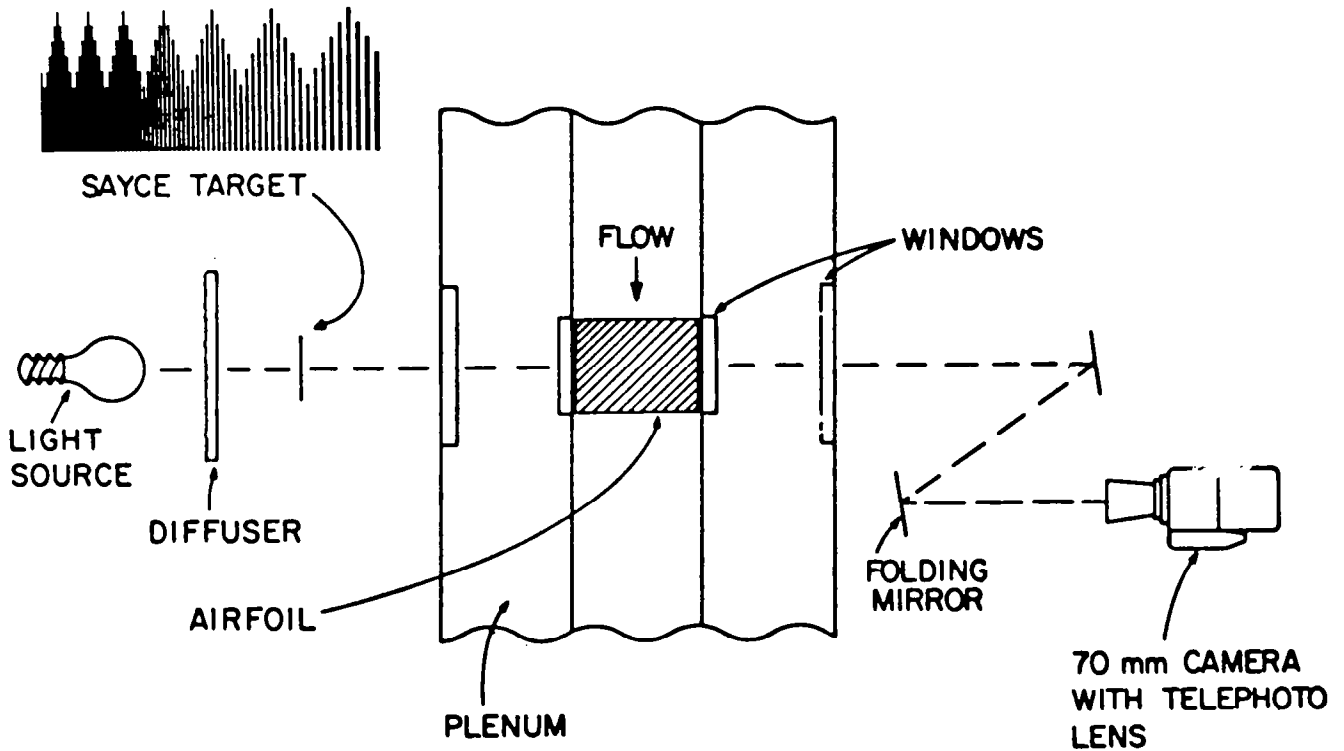

Figure 4

PHOTOGRAPHS OF SAYCE TARGETS

    An ideal system would resolve even the finest lines. The upper photo in figure 5 represents the mildest flow condition encountered in this facility while the lower shot represents a temperature induced density increase of only 2.5. The coarsest grid lines are barely discernible even at these modest conditions.
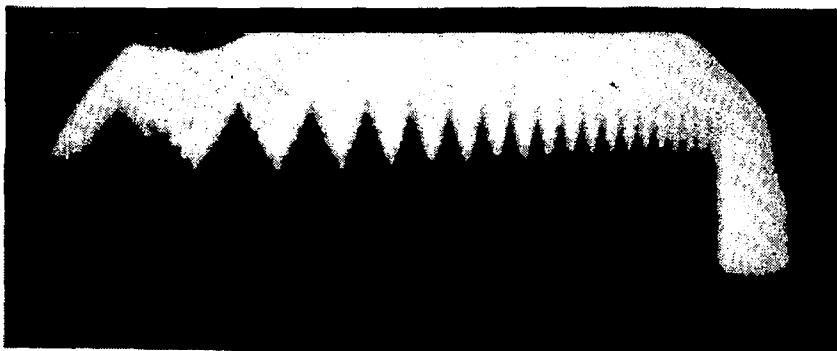
$P = 1.2$ ATM.

$M = 0.65$

$\alpha = 6^0$

250 K

100 K

Figure 5

DENSITOMETER TRACES OF SAYCE TARGETS

    Densitometer traces corresponding to figure 5 are shown in figure 6. The top trace is for 1.2 atmospheres and 250 K while the lower is for 1.2 atmospheres and 100 K. The vestiges of a shock can be seen against the Sayce background as a dip in the modulation near the coarse edge of the target.
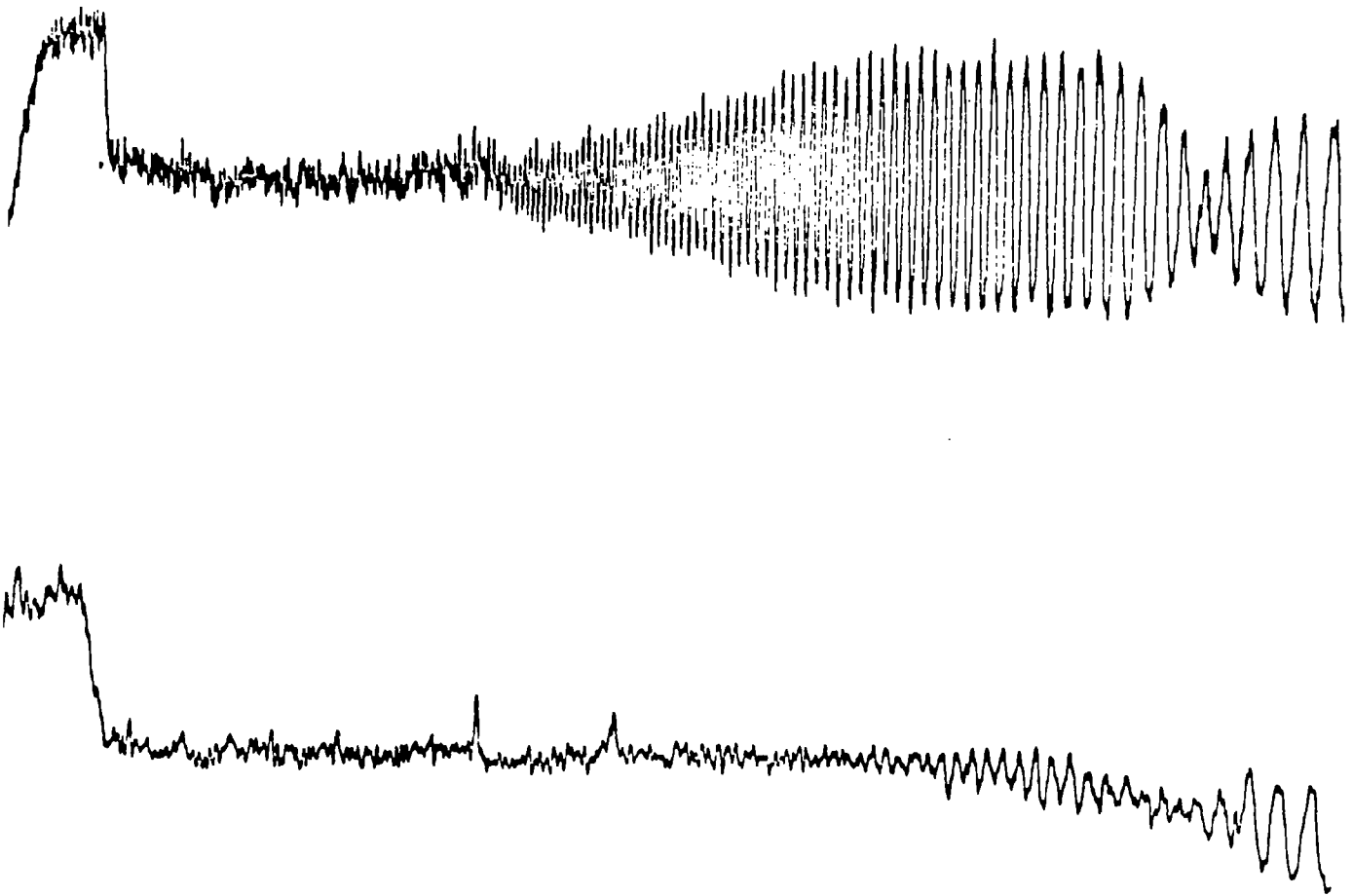
Figure 6

PHOTOGRAPHY THROUGH THE TOP WINDOW

To more closely approximate the model deformation format, a target was contact printed on stripping film and the film appliquéd to the surface of an airfoil. The target was photographed using the relay system shown in figure 7.

FLIP MIRROR

70 mm CAMERA WITH CLOSE-UP ADAPTER

VIDICON

FIELD LENS

RELAY LENS ASSEMBLY

TEST SECTION

PLENUM

FLOW PERPENDICULAR TO FIGURE

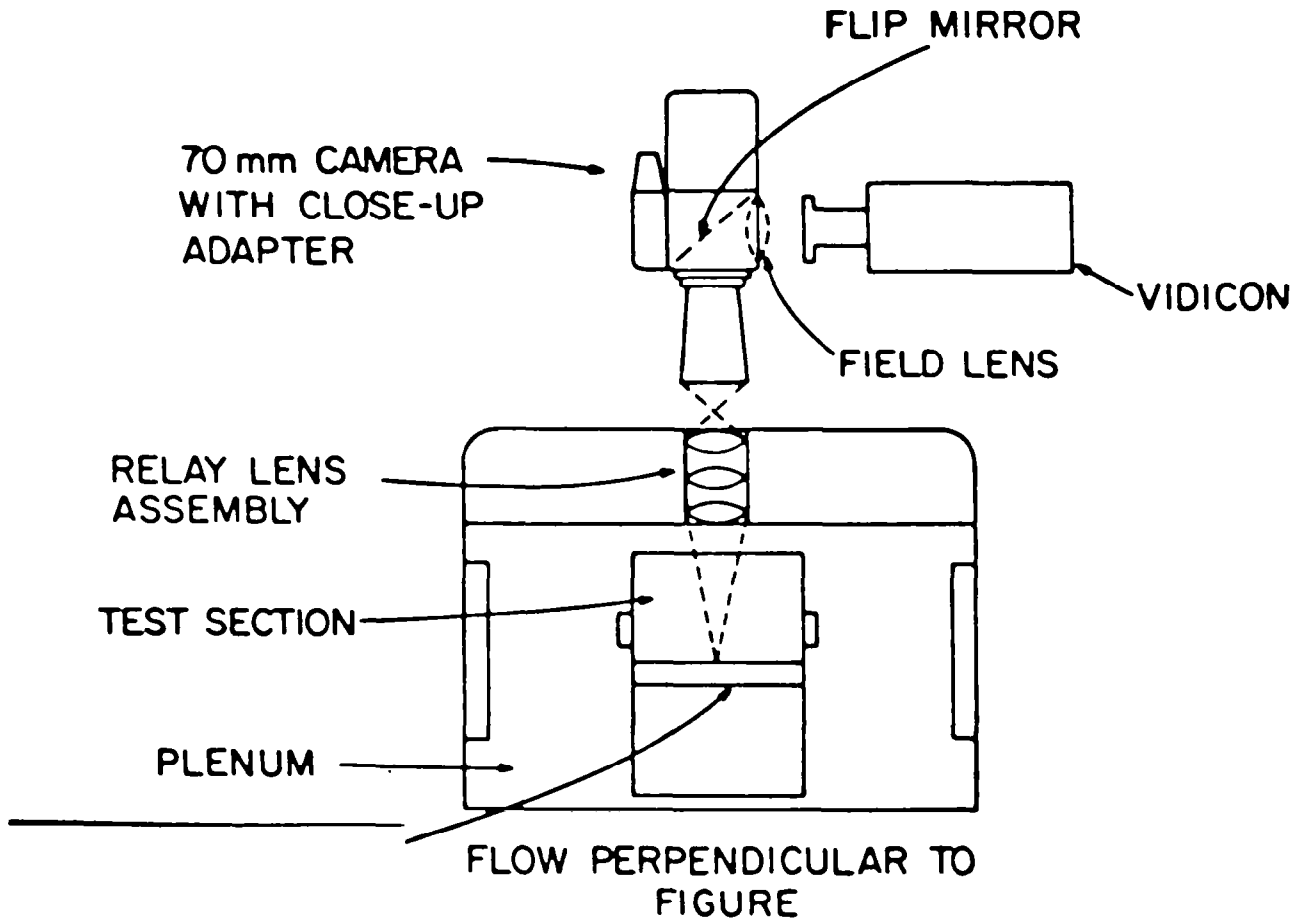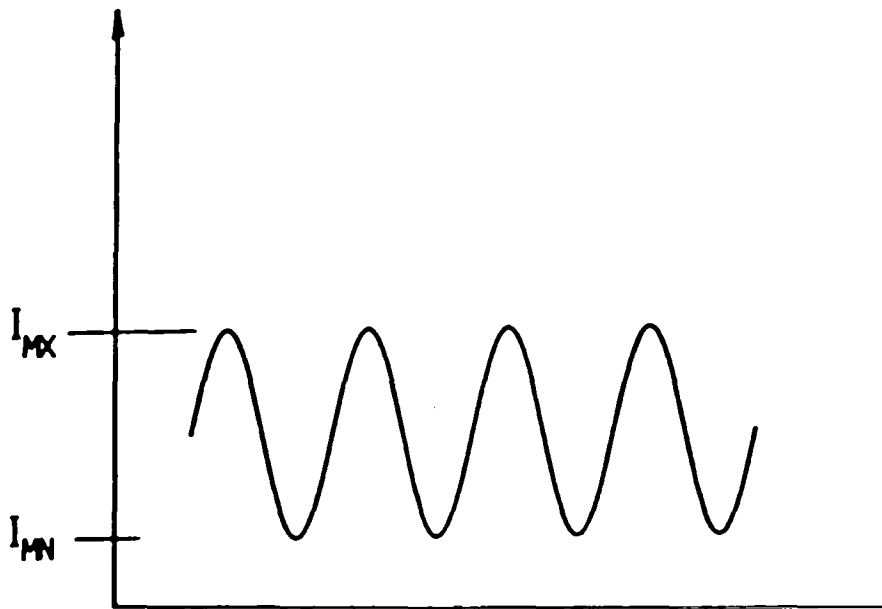Figure 7

DEFINITION OF THE MODULATION FUNCTION

The photos made using the relay system were remarkably crisp. A quantitative evaluation was made by plotting the response as a function of spatial frequency. The contrast as defined in figure 8 was measured. If I_{mn} is zero then $V = 1.0$ and you have a perfect contrast whereas if I_{mn} equals I_{mx} there is a complete redistribution of energy to a dc value, the contrast is zero and results in complete information loss.

$$V = \frac{I_{MX} - I_{MN}}{I_{MX} + I_{MN}}$$

Figure 8

RESPONSE FUNCTIONS

Response functions for two test conditions obtained using both top and side viewing configurations are shown in figure 9. Some degradation is expected with increased density but the large discrepancy between top and side results were puzzling and prompted further investigation. The response is defined as the ratio of measured to reference modulation.
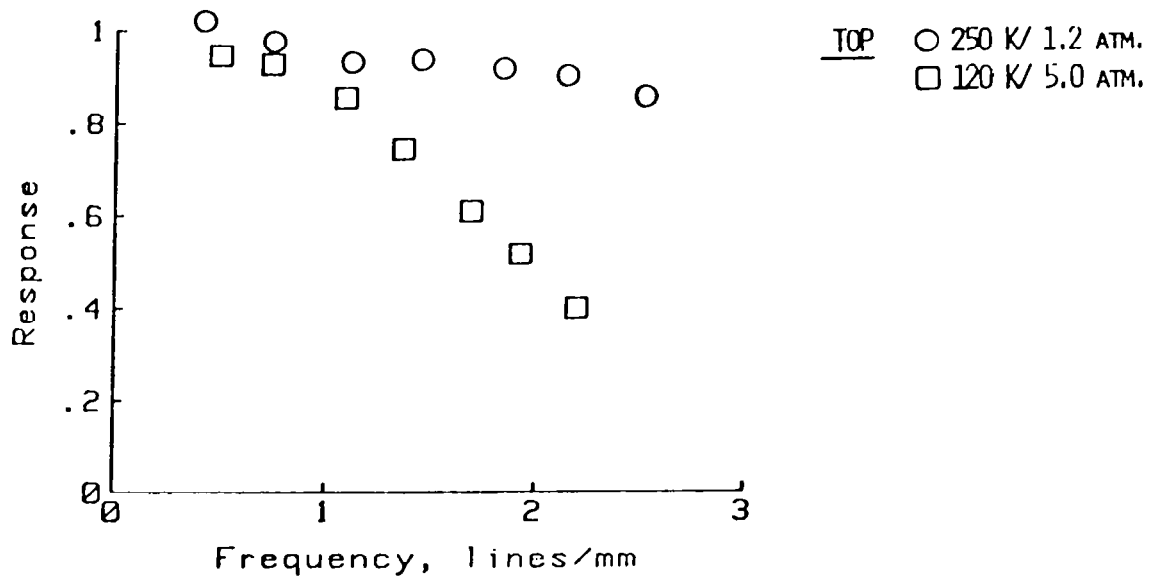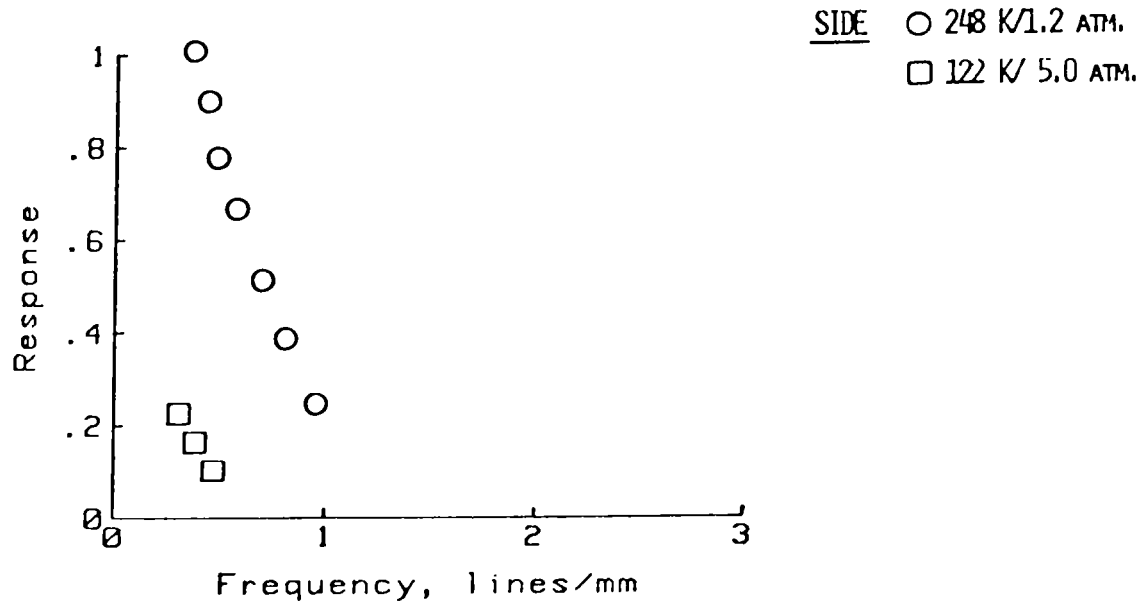
SIDE ○ 248 K/1.2 ATM.
      □ 122 K/ 5.0 ATM.

Response

Frequency, lines/mm

TOP ○ 250 K/ 1.2 ATM.
     □ 120 K/ 5.0 ATM.

Response

Frequency, lines/mm

Figure 9

REPEAT OF SIDE WINDOW EXPERIMENT WITH EACH WINDOW TARGETTED

The discrepancy prompted a return to the pod experiment with targets affixed to each window (shown shaded in figure 10) and the camera mounted on a track to allow viewing of each target individually at each tunnel condition. The critical station proved to be that nearest the camera and outside of the flow. The effect was attributed to vibration which was progressively worse as the tunnel approached its operating envelope.
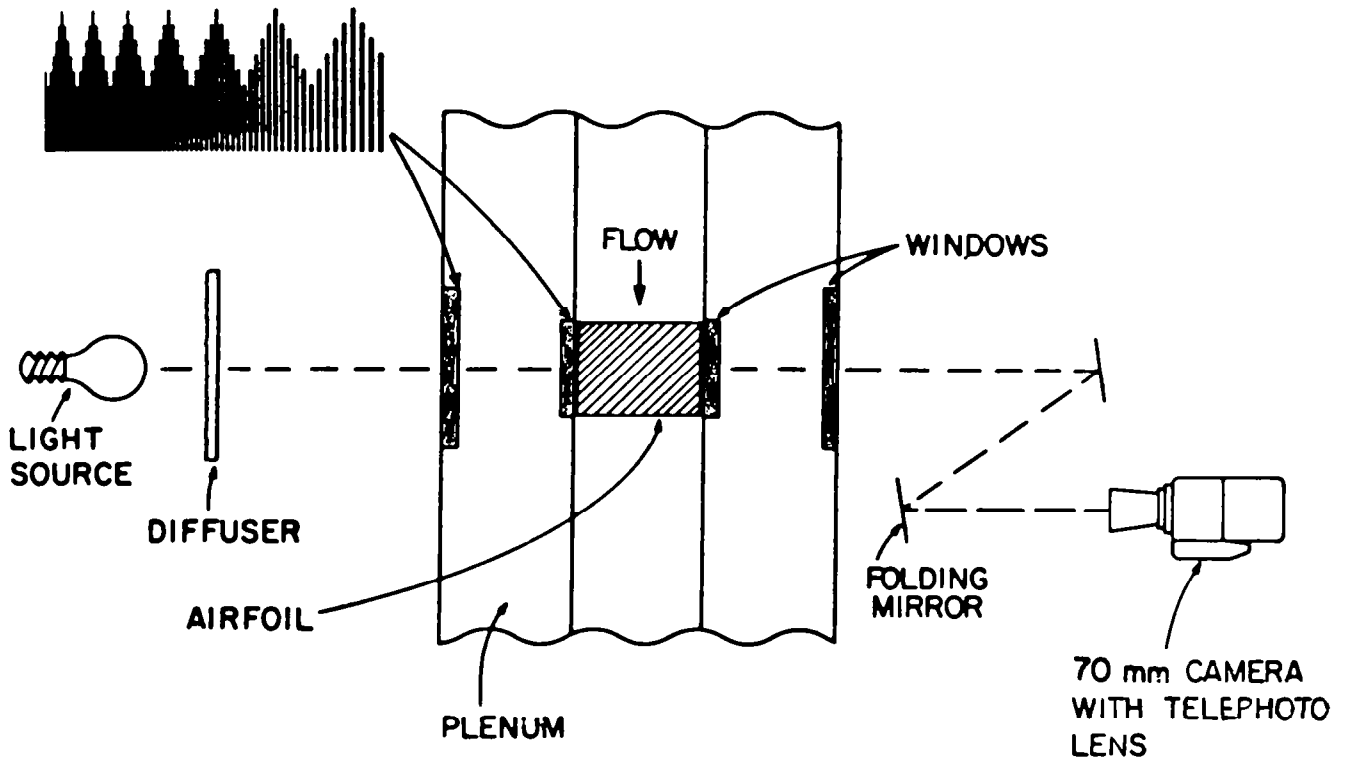

Figure 10

REVISED RESPONSE FUNCTIONS

When several independent mechanisms contribute, their MTF's multiply together to obtain the system MTF. The transfer function relating to vibration could be determined by examining the data for the nearest station to the camera since it was outside the flow. When this information was used to correct the earlier results (solid symbols) the data became consistent with that for the top shots as shown in figure 11.
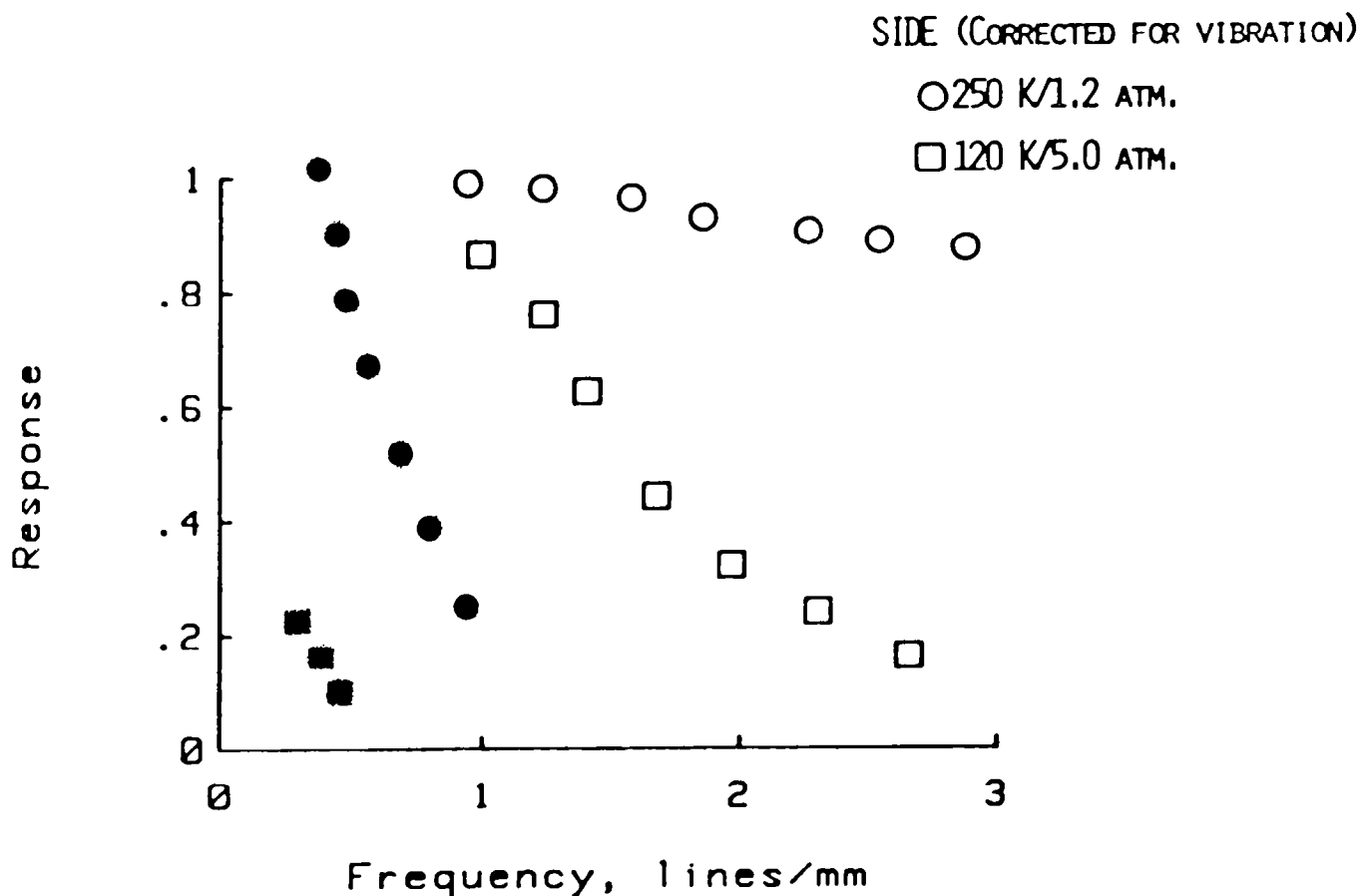

Figure 11

MODELLING IMAGE DEGRADATION USING EXPERIMENTAL RESULTS

The energy distribution for an ideal target can be represented by a step function as shown in figure 12. This distribution can be decomposed in a Fourier series. Each of these coefficients is tied to a spatial frequency. If the MTF is unity for a particular frequency then the corresponding coefficient is unchanged. Otherwise it is multiplied by the fractional response thus attenuating its contribution. If the square wave is reconstructed with coefficients modified by the MTF depicted by open squares in figure 11 the result is shown as the attenuated and extended curve in figure 12. The energy is redistributed and the contrast reduced. Note that this was for a flow-off condition and therefore does not include turbulence effects.
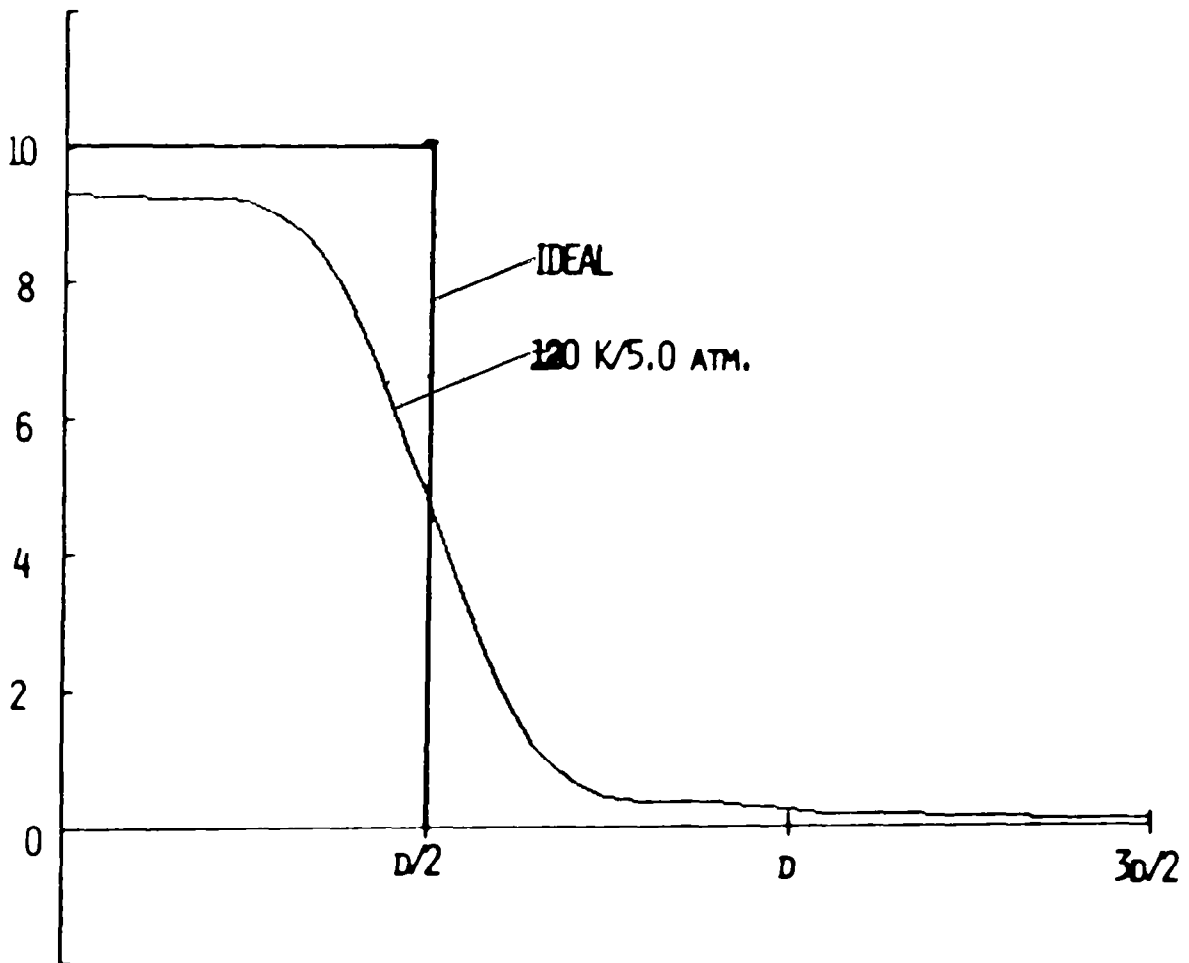

Figure 12

SUMMARY COMMENTS

DEGRADATION DUE TO INCREASED DENSITY, THOUGH MEASURABLE, SHOULD NOT IMPACT THE MODEL DEFORMATION APPROACHES.

EFFECTS OF TURBULENT BOUNDARY LAYERS ARE UNAVOIDABLE AND WILL BE ASSESSED ON SITE.

VIBRATIONAL DEGRADATION COULD DOMINATE THE PREVIOUS EFFECTS AND WILL BE MONITORED AND GUARDED AGAINST BY DESIGN OF CAMERA ENCLOSURES.